J Computer-Aided Mater Des
DOI 10.1007/s10820-006-9034-9

Dielectric properties of nanoscale multi-component systems: A first principles computational study

N. Shi · R. Ramprasad

Received: 3 June 2006 / Accepted: 1 September 2006
© Springer Science+Business Media B.V. 2007

Abstract A new method has been developed within the framework of density functional theory to aid in the study of the dielectric properties of multi-component systems, with explicit treatment of surface and interface effects. Specially, we have determined the position dependent dielectric constant profiles for Si–SiO_2 and SiO_2-polymer systems. We find that at regions close to surfaces and interfaces, the dielectric constant is enhanced compared to the corresponding bulk values. In interior regions, the dielectric constant approaches the corresponding bulk values. The calculated optical and static dielectric constant values of these systems are in excellent agreement with experimental results, and other more involved computational treatments.

Keywords Local dielectric · Permitivity · Density functional theory · Heterostructures

1 Introduction

In recent years, dielectric materials of nanoscale dimensions have aroused considerable interest. It is well known that the high energy density capacitor industry is currently considering dielectric composites with a polymer host matrix filled with nano-platelets of inorganic dielectric materials [1,2]. Also, for many present day microelectronics applications, thin film morphologies are required [3]. In both these cases, as the system sizes reach the nanoscale regime, polarization at the interfaces between the dielectric and other materials will be dominant in determining the dielectric properties [4,5]. While several sophisticated first principles methods have been employed to calculate the dielectric constant of bulk materials [6–8], these methods do not allow for a practical characterization of such surface and interface effects.

N. Shi · R. Ramprasad (✉)
Department of Materials Science and Engineering, Institute of Materials Science, University of Connecticut, 97 N. Eagleville Road, Storrs, CT, 06269, USA
e-mail: rampi@ims.uconn.edu

The primary goal of this work is to introduce a new scheme within density functional theory to determine position dependent dielectric permittivity profiles and to determine the extent to which surfaces and interfaces modify the polarization and the dielectric constant of systems with one of their dimensions in the nano regime.

2 Computational details

All calculations were performed using the local density approximation (LDA) within DFT [10] as implemented in the local orbital SIESTA code [11]. Norm-conserving non-local pseudopotentials of the Troullier–Martins type were used to describe all the elements. The atomic configuration [Ne]$3s^2 3p^2$ was used for the Si pseudopotential, [He]$2s^2 2p^4$ for the O pseudopotential, [He]$2s^4$ for C pesudopotential, and [H] for H pseudopotential. A double-zeta plus polarization (DZP) basis set was used for all calculations. The equilibrium positions of the atoms were determined by requiring the forces on each atom to be smaller than 0.01 eV/ Å.

In this work, two interfaces are considered: one between SiO_2 in the α-quartz phase and Si, and the other between SiO_2 in the β-cristobalite phase and a $C_{12}H_{26}$ molecule simulating a polymer chain. The bulk properties of each of the component were well predicted by our computational treatment. [12,13].

3 Theory of "local" dielectric constant

Our prior calculations of the dielectric properties of ultrathin dielectric slabs indicated the need for a careful treatment of surface effects. For instance, Fig. 1 shows the dipole moment per unit area, m_0, induced in a slab of SiO_2 in the α-quartz phase due to an electric field of 0.1 V/ Å along the slab normal, as a function of the slab thickness. Data corresponding to two situations are shown: the "optical" (or high frequency) response of the system, obtained when the ionic positions were fixed at their field free equilibrium positions, and the "static" (or low frequency) response,

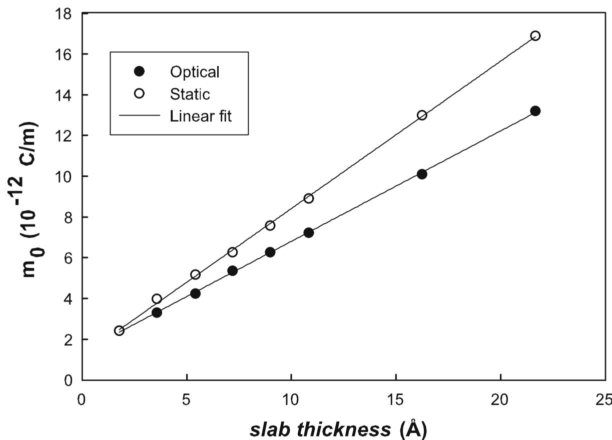

Fig. 1 Dependence of the total dipole moment density of an isolated SiO_2 slab on the slab thickness

when both the ionic and electronic degrees of freedom were allowed to respond to the external electric field. For further details concerning these calculation can be found elsewhere [12].

The bulk polarization, $P_{\rm bulk}$, obtained as the slope of the lines in Fig. 1 can be used to determine the bulk dielectric constant ε, using:

$$\varepsilon = \frac{\varepsilon_0 E_{\rm ext}}{\varepsilon_0 E_{\rm ext} - P_{\rm bulk}} \tag{1}$$

where ϵ_0 and $E_{\rm ext}$ are the permittivity of free space and the external field, respectively. The calculated electronic and total dielectric constants using this method are 2.54 and 4.69 for α-quartz, respectively, both of which compare very well with experimental results 2.40 and 4.52 [14,15]. The y-intercept of the curves in Fig. 1 represent the surface contribution to the polarization. This effect has been observed for HfO_2 slabs as well [9].

In order to further determine the extent to which such surface effects modify the polarization and the dielectric constant of systems, we present a theory to determine atomic-scale dielectric permittivity profiles across interfaces between insulators. A local permittivity function is introduced to describe variations of the dielectric response over length scales of the order of interatomic distances, which can conveniently be calculated from the local charge density profile as follows.

As we are interested in defining a dielectric permittivity which varies in the z direction (defined as the normal to a surface or interface), we can use the 1-dimensional version of the Gauss relation that relates the microscopic polarization $\bar{p}$(z) and the induced charge density $\bar{\rho}_{\rm ind}$(z):

$$\frac{d}{dz}\bar{p}(z) = -\bar{\rho}_{\rm ind}(z) \tag{2}$$

where the bars indicate averages over the xy planes. In this work, we evaluated the induced charge density $\bar{\rho}_{\rm ind}$(z) by applying finite electric fields with $\pm 0.02\,$V/Å and taking the finite differences of the resulting charge densities for the positive and negative fields. The solution for Eq. 1 is given by:

$$\bar{p}(z) = \bar{p}_{-\infty} - \int_{-\infty}^{z} \bar{\rho}_{\rm ind}(\acute{z})d\acute{z} \tag{3}$$

For our slab system, the constant $\bar{p}_{-\infty}$ can be set to zero as it corresponds to the polarization at $-\infty$, a region where charge density is zero.

The calculated polarization profile can be used to determine the position dependent dielectric constant, $\epsilon(z)$ using:

$$\varepsilon(z) = \frac{\varepsilon_0 E_{\rm ext}}{\varepsilon_0 E_{\rm ext} - \overline{P}(z)} \tag{4}$$

Using $\bar{p}$ corresponding to the situation when the atoms were frozen at the field free positions but the electrons allowed to relax would result in the electronic (or optical) part of the dielectric constant, whereas using $\bar{p}$ obtained by allowing both the atoms

and electrons to relax to their field induced equilibrium positions would yield the total (or static) dielectric constant.

4 Results

Using this new method, we can relate variations of the microscopic dielectric response to specific features of the local bonding arrangement. The potential of this theory is illustrated through application to two different interface systems: Si–SiO_2 and SiO_2-polymer chain. In both cases, the 2-component sandwich is separated from its periodic images inherent in slab supercell calculations by a vacuum region, as shown in Fig. 2 and 3.

The Si/SiO_2 interface and surface have been studied for many decades due to their importance in metal-oxide-semiconductor field effect transistors. In this study we examine the dielectric constant profile across a Si/SiO_2 interface. We consider the Si and SiO_2 regions to be crystalline, with the latter having the β-cristobalite structure in the interface models.

In order to obtain a structural transition without coordination defects between the silicon and its oxide in our model interface, we adopt a bridging oxygen model (BOM) for the interface described earlier. The thickness of the suboxide region within this model is about 3 Å, and all the partial oxidation states of Si (namely, Si, Si + 1, Si + 2, and Si + 3) appear in equal amounts in the suboxide region.

Figure 2 shows a schematic of the Si-β-cristobalite SiO_2 interface (above) and the dielectric constant profile as a function of position along the slab normal (below). The thickness of the Si and SiO_2 layers were 10.96 Å and 14.70 Å, respectively. As shown in these figures, for the combined 2-component system, the dielectric properties in the

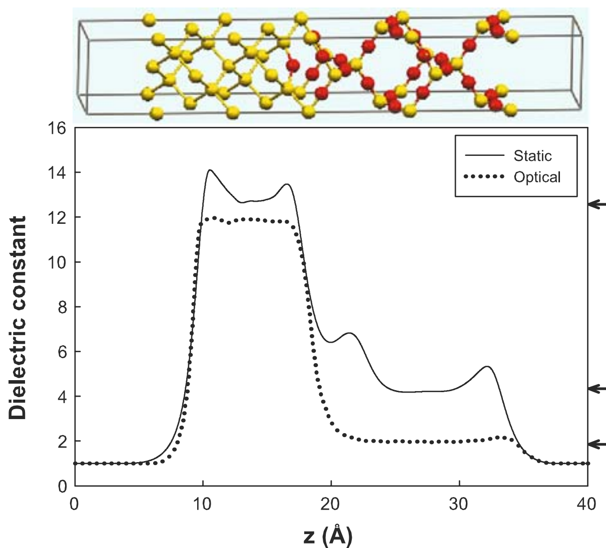

Fig. 2 Above: Schematic of Si–SiO_2 interface; Si and O atoms are shown in yellow and red colors, respectively. Below: the dielectric constant along a direction normal to the interface; arrows indicates the experimental values of the bulk static and optical dielectric constant of Si and SiO_2

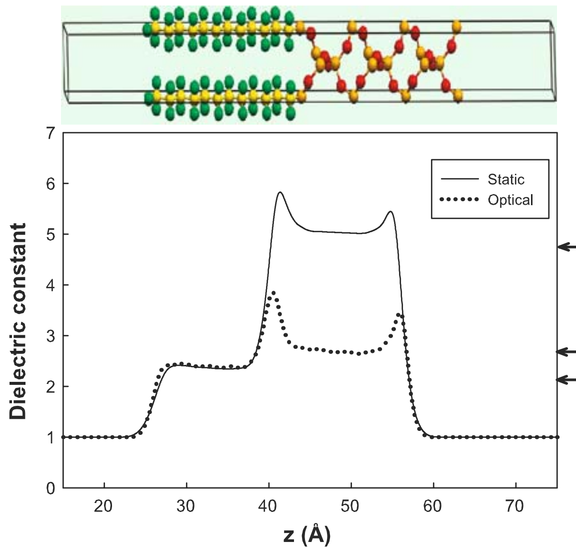

Fig. 3 Above: Schematic of $C_{12}H_{26}$–SiO_2 interface; C, H, Si and O atoms are shown in yellow, green, red and purple colors, respectively. Below: the dielectric constant along a direction normal to the interface; arrows indicates the experimental values of the bulk constants of polymer and SiO_2

interior of the SiO_2 and Si regions match well with the corresponding experimental single component bulk values. However, at the interfaces and surfaces, we find that there is an enhancement of the dielectric constant, compared to those of the bulk and the oxide free surface. The deviation at the interface is due to the Si atoms that exist in partial oxidation states as pointed out earlier [16], and is also consistent with prior experimental [17] results.

We then studied the combined two-component SiO_2-polymer chain system, whose geometry is shown in Fig. 3 (above). Here, SiO_2 was assumed to be in the α-quartz phase of thickness 15.96 Å, and the polymer chain was approximated by a $C_{12}H_{26}$ molecule. The lower part of Fig. 3 shows the dielectric constant as a function of position along the slab surface normal for SiO_2-polymer system. We observe similar behavior of the dielectric constants as with the Si–SiO_2 interface. The dielectric constants in the interior of the SiO_2 and $C_{12}H_{26}$ chain regions match well with the corresponding experimental single component bulk values (indicated by arrows in Fig. 3) and there is an enhancement of the dielectric constant, compared to the 1-component results at the interfaces and surfaces. In contrast to the Si–SiO_2 interface, the enhancement in the dielectric constant at the polymer-SiO_2 interface is almost entirely in the SiO_2 side of the interface. Analysis of the Mulliken charges of the atoms indicates that C atoms closest to the interface are in their nominal oxidation states (i.e., in oxidation states similar to that of C atoms in the interior of the polymer chain), whereas the Si and O atoms close to the interface are in varying oxidation states similar to that in the Si–SiO_2 case. This is consistent with the deviation of the dielectric constant from the corresponding bulk value only on the SiO_2 side of the interface. It is likely that such a behavior is specific to the polymer-oxide interface model chosen here. Nevertheless, an enhancement of the dielectric constant at the SiO_2 side of the interface is expected to occur in general, as the Si–O bond is more polar than the bonds in polymer chains.

Although a quantitative comparison with experiments concerning the enhancement in dielectric constants can not be performed due to the unavailability of specific experiment data, it is worth mentioning that the calculated enhancement at the interface is consistent with recent experimental work on polymer-oxide composites, which display effective permittivities noticeably higher than that expected given the permittivity of the corresponding single component bulk values [2].

While we have demonstrated the applicability of our method for just a few restricted situations, we believe that this simple procedure for calculating the position dependent dielectric properties has a broader appeal. The present approach can be systematically used in a study of the impact of a wide variety of interfaces and other types of atomic level disorder on the dielectric properties.

5 Summary

A new method has been developed within the framework of DFT to aid in the study of the dielectric properties of multi-component systems, with explicit treatment of surface and interface effects. Specially, we have determined the position dependent dielectirc constant profiles for Si–SiO_2 and SiO_2-polymer systems. We find that at regions close to surfaces and interfaces, the dielectric constant is enhanced compared to the corresponding bulk values. In interior regions, the dielectric constant approaches the corresponding bulk values. The calculated optical and static constant values of these systems are in excellent agreement with experimental results, and other more involved computational treatments.

These calculations form the groundwork for a more thorough analysis of the impact of surfaces, interfaces and atomic level defects on the dielectric properties of a wide variety of nanostructured systems.

Acknowledgements Partial support of this work by grants from the ACS Petroleum Research Fund and the Office of Naval Research is gratefully acknowledged.

References

1. Rao, Y., Wong, C.P.: Material characterization of a high-dielectric-constant polymer-ceramic composite for embedded capacitor for RF applications, *J. Appl. Polym. Sci.* **92**, 2228 (2004)
2. Murugarai, P., Mainwaring, D., Mora-Huertas, N.: Dielectric enhancement in polymer-nanoparticle composites through interphase polarizability, *J. Appl. Phys.* **98**, 054304 (2005)
3. Wilk, G.D., Wallace, R.M., Anthony, J.M.: High-κ gate dielectrics: Current status and materials properties considerations, *J. Appl. Phys.* **89**, 5243 (2001)
4. Perkins, C.M., Triplett, B.B., Mclntyre, P.C., Saraswat, K.C., Haukka, S., Touminen, M.: Electrical and materials properties of ZrO_2 gate dielectrics grown by atomic layer chemical vapor deposition, *Appl. Phys. Lett.* **78**, 2357 (2000)
5. Chang, H.S.,et al.: Measurement of the physical and electrical thickness of ultrathin gate oxides, *J. Vac. Sci. Technol. B.* **20**, 1836 (2002)
6. Rignanese, G.-M., Detraux, F., Gonze, X., Pasquarello, A.: First-principles study of dynamical and dielectric properties of tetragonal zirconia, *Phys. Rev. B* **64**, 134301 (2001)
7. Zhao, X.Y., Vanderbilt, D.: First-principles study of structural, vibrational, and lattice dielectric properties of hafnium oxide, *Phys. Rev. B* **65**, 233106 (2002)
8. King-Smith, R.D., Vanderbilt, D.: Theory of polarization of crystalline solids, *Phys. Rev. B* **47**, 1651 (1993)
9. Ramprasad, R., Shi, N.: Dielectric properties of nanoscale HfO_2 slabs, *Phys. Rev. B* **72**, 052107 (2005)

10. Martin, R.: Electronic Structure: Basic Theory and Practical Methods. Cambridge University Press, New York (2004)
11. Soler, J.M., Artacho, E., Gale, J., Garcia, A., Junquera, J., Ordejon, P., Sanchez-Portal, D.: The SIESTA method for *ab initio* order-N materials simulation, *J. Phys.: Condens. Matter* **14**, 2745 (2002)
12. Shi, N., Ramprasad, R.: Dielectric properties of ultrathin SiO_2 slabs, *Appl. Phys. Lett.* **87**, 262102 (2005)
13. Shi, N., Ramprasad, R.: Atomic-scale dielectric permittivity profiles in slabs and multilayers, *Phys. Rev. B* **74**, 045318 (2006)
14. Wolf, W.L., Stanley, S.B., McCarthy, K.A.: American Institute of Physics Handbook, p.24. McGraw-Hill, New York (1963)
15. Gervais, F., Piriou, B.: Temperature dependence of transverse and longitudinal optic modes in the α and β phases of quartz, *Phys. Rev. B* **11**, 3944 (1975)
16. Giustino, F., Umari, P., Pasquarello, A.: Dielectric Discontinuity at Interfaces in the Atomic-Scale Limit: Permittivity of Ultrathin Oxide Films on Silicon, *Phys. Rev. Lett.* **91**, 267601 (2003)
17. Perkins, C.M., Triplett, B.B., Mclntyre, P.C., Saraswat, K.C., Haukka, S., Tuominen, M.: Electrical and materials properties of ZrO_2 gate dielectrics grown by atomic layer chemical vapor deposition, *Appl. Phys. Lett.* **78**, 2357 (2001)